Field Performance Testing of a Floating Tidal Energy Platform - Part 1: Power Performance

Ralf Starzmann[#1], Inga Goebel[#], Penny Jeffcoate[*2]

[#]SCHOTTEL Hydro GmbH, Spay, Germany

[1]RStarzmann@schottel.de

[*]Sustainable Marine Energy Ltd, Edinburgh, U.K.

[2]penny.jeffcoate@sustainablemarine.com

***Abstract* — SCHOTTEL HYDRO has developed the SCHOTTEL Instream Turbine (SIT). Four SITs had been mounted on Sustainable Marine Energy's floating surface platform PLAT-I, with a combined platform rated power of 280kW. The PLAT-I platform has been undergoing field performance testing in Scotland to determine the power performance of the individual turbines according to IEC62600-200.**

Time series as well as processed performance data shows a high spatial variation of the inflow across the platform and hence a high dependency on the flow speed measurement location. The turbines power performance is found to be in line with design predictions, whereas the thrust loads measured are lower than the predictions.

***Keywords*—Tidal energy; SCHOTTEL Instream Turbine; Performance Assessment; Floating**

NOMENCLATURE

ADCP	Acoustic Doppler Current Profiler
ECM	Electromagentic Current Meter
IEC	International Electrotechnical Commission
PLAT-I	PLATform for Inshore Energy
PLAT-O	PLATform for Offshore Energy
TSR	Tip speed ratio
TEC	Tidal Energy Converter
SIT	SCHOTTEL Instream Turbine
SDM	SIT Deployment Module

I. INTRODUCTION

Validating the power performance of a tidal turbine is a key element in moving forward towards commercialisation for the tidal energy sector. This includes both performance prediction during the design phase as well as field measurements. During the design phase of turbine development blade-element momentum models and model scale tank tests are widely used [1]. For full-scale operational tests guidelines and test methodology are set out in IEC62600-200, the technical specification for Tidal Energy Converter (TEC) power performance assessment [1]; this standard has been used previously to assess the performance of seabed mounted tidal turbines [3].

Comprehensive testing has been carried out and published for the first generation SCHOTTEL Instream Turbine (SIT). These include full-scale pushing tests in Rotterdam harbour [4] and moored tests using a floating platform at Queen's University Belfast's Tidal Test Site in Strangford Lough [5]. A comparison of both data sets showed comparable power output and performance curves for both the steady and turbulent tidal tests [6].

Performance prediction using a blade-element momentum model has been validated for the second generation SIT 250 blade geometry. This included towing tank as well as cavitation tunnel data and showed very good agreement for power and thrust coefficients, as well as the cavitation inception bucket over a wide range of tip speed ratios **Fehler! Verweisquelle konnte nicht gefunden werden.**.

This paper presents results for SCHOTTEL HYDRO´s current SIT 250 turbine design at full-scale in a tidal environment. Sustainable Marine Energy's PLAT-I platform has four SIT250 turbines and was recently deployed in a field test. The testing method and analysis of turbine performance characterisation were guided by the IEC62600-200 Technical Specification for Tidal Energy Converter (TEC) power performance assessment [2]. The overall objective of this work is a full-scale assessment of the turbines during the Sea Acceptance Tests of PLAT-I at Connel, Oban, Scotland. Further information on the platform results can be found in Part 2 [7].

II. FLOATING TIDAL ENERGY SYSTEM

A. SIT 250 Turbine System

SCHOTTEL's commercial SIT 250 is a horizontal axis free-flow turbine (Figure 1). SIT is a passive-adaptive, three-bladed rotor, with a planetary gearbox, an asynchronous generator and a hydraulic brake. The system is cooled by ambient water. The full-scale SIT 250 is currently available in two rotor diameters: 4m and 6.3m. For the tests presented in this work four turbines with a 4m rotor were used.

Figure 1: SIT 250 turbine

Figure 2 shows the electrical setup during the tests. Four inverters (one for each turbine) are linked together to a common DC-Link. Each turbine is individually controlled by its own inverter. The generated power from each turbine is fed back across an immersion heater AC load bank, using a regenerative unit of 300kW rated power. The regenerative unit is equipped with a software tool which controls the load to the load bank. Another bi-directional active front end unit is connected to the same DC-bus to provide voltage and power for the auxiliary network. An auxiliary transformer is used to decouple the regenerative unit from the network. Since the platform wasn’t connected to the grid during the testing a small diesel generator was connected to the auxiliary network to start up the system and simulate the grid.

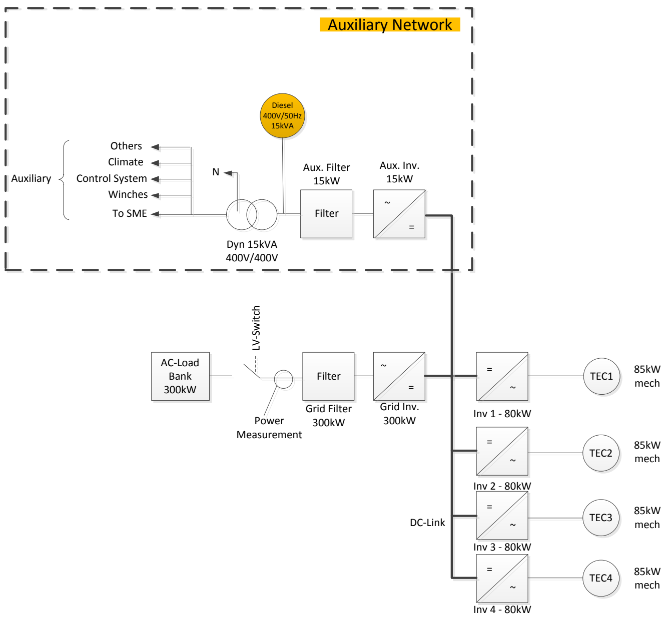

Figure 2: SIT 250 electrical setup

B. PLAT-I Floating Platform

PLAT-I is a three-hulled tidal energy platform that hosts the SIT 250 turbines. The turbines are suspended from the cross-deck, via lifting support structures called SIT Deployment Modules (SDMs). During normal operation, or when parked, the turbines are in the down configuration, but they can be lifted clear of the water for operations and maintenance, Figure 3.

Figure 3: SIT 250s and SDMs in maintenance position

The platform self-aligns to incoming flow via a mooring turret, Figure 4, which is connected to a geostationary mooring spread. During the Sea Acceptance Trials of PLAT-I at Connel, Oban, Scotland the system was moored via a four-point spread and Raptor rock anchors (detailed in Part 2 [7]).

Figure 4: PLAT-I in operation as deployed in Connel, Oban

The turbines operate in both clockwise and counter-clockwise direction (looking upstream), as shown in Figure 5. The turbines are named SIT1 to SIT4 from Port to Starboard. The hub deployment depth is 4.7m.

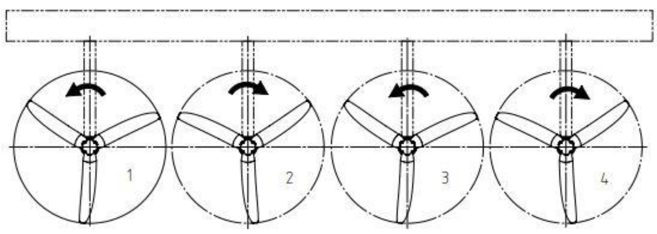

Figure 5: Schematic SIT 250 configuration on PLAT-I

III. Field Testing

PLAT-I was deployed in Connel, Oban for field tests. During this trial the platform and its turbines were tested in various modes and operational states.

A. Test Site (Connel, Scotland)

The test site is located at Connel, Oban at the mouth of Loch Etive in Scotland. This is a sheltered sea loch with a large tidal zone, creating strong flows but minimal wave conditions. The site is only exposed to the West, but surrounding coast and islands reduce the fetch and therefore wave climate.

The site at Connel is ideal for trial deployments, as the flow speed on the ebb is driven by a jet formed by the Falls of Lora. This gives very localised fast flow, but with calm surrounding conditions for access and support infrastructure. Additionally, the flood tide is very benign, giving long operational windows for maintenance.

The tidal jet on the ebb creates a strong localised flow but does result in high temporal and spatial variation in flow speed, Figure 6. This gives a very rigorous test environment for the multi-turbine platform.

Figure 6: PLAT-I position in the Falls of Lora

B. Instrumentation

Instruments were mounted on the platform to measure the current velocity, turbine performance and reaction force at the SDM (due to rotor thrust and SDM drag). These are detailed in Table 1. The rotor thrust was derived by resolving the forces acting on the SDM, including SDM drag, SDM and SIT masses, and rotor thrust, see [7] for more details.

The IEC standard [2] defines a bed mounted current profiler (ADCP) as the preferred current velocity measurement device, as well its postion relative to the energy extraction plane. In this work a Valeport Electromagentic Current Meter (ECM) close to the water surface is used, which only provides a single measurement point, rather than a power-weighted average of the flow at hub height as derived from a flow profile as per IEC reccomondation. Though this does not comply with IEC recommendation the IEC method will be followed where posible to validate performance.

TABLE 1
Test Instrumentation

Parameter	Instrument	Location	Label
Power	S120 SIEMENS Inverter	Control Container	3
Torque	S120 SIEMENS Inverter	Control Container	3
Rot. Speed	S120 SIEMENS Inverter	Control Container	3
Velocity	Valeport Electromagnetic Current Meter	Upstream from SIT2 6.1m, 27cm below water surface	2
Reaction force at pins (Thrust)	LCM Load Pin	Lower connection point between SDM and crossdeck structure	1

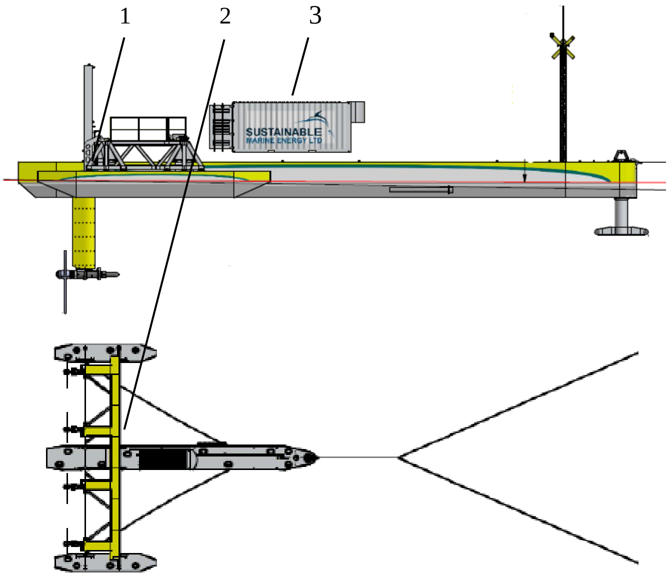

Figure 7: PLAT-I with instrumentation locations

In order to quantify the measurement position of the current meter relative to a multiple turbine system the equivalent diameter D_E is used, where f is turbine number and D is diameter in metres:

$$D_E = \left(\sum_f^F D_f^2\right)^{1/2}. \quad (1)$$

The effective diameter, D_E, for four 4m rotors is 8m. The position of the Valeport ECM is compared with the target position as defined in the IEC standard in Table 2 below; the position relative to the effective diameter of both the four turbine arrangement and a single turbine (SIT2) are shown. The lateral distance is greater than the platform target because the unit was mounted upstream from a single turbine (SIT2). The axial distance is less than the target distance due to mounting restrictions. Besides the Valeport current meter, a vessel mounted ADCP, a bed mounted ADCP, and an ADV were also deployed, however these are not used in this paper.

The vessel ADCP was mounted as close to these target measurement parameters as possible.

TABLE 2
Valeport Current Meter(ECM) position relative to turbines

	Distance y from principal axis of energy capture	**Distance x from energy extraction plane**
IEC TS 62600-200	$y \leq 0.5D_E$	$2D_E \leq x \leq 5D_E$
Platform, D_E = 8m	y = 0.43 D_E	x = 0.77D_E
SIT2, D_E = 4m	y = 0.02 D_E	x = 1.53 D_E

C. Tests

The platform was installed at the end of November 2017. Many different test configurations and operational parameters were assessed during the field tests. Test data presented in this work will cover the some of the test period from 16th December to 11th January 2018 and 2nd February to 3rd March 2018.

IV. DATA PROCESSING & TURBINE PARAMETERS

A. Post-Processing

Time series results were produced using the raw data. Various sampling rates had been used during the data collection for different instruments and test objectives, however all data in this work was reduced to 1Hz. All data was recorded synchronously and no filtering was applied to the data sets. All post-processing was applied to the data as per IEC [1]. Further detail and equations can be found in the reference document, though key equations will be presented here. The IEC suggests using an averaging period between 2 and 10 min; the data presented here has been 2 min averaged. In general, the following steps are performed using the bin methodology:

1. Calculate the mean recorded current velocity of a 2min data set, as per equation 2, where *i* is the flow velocity bin, *j* is the instantaneous velocity data point, *L* is the number of instantaneous velocity data points, and *n* is the number of data points in a velocity bin.
2.

$$\bar{U}_{i,n} = \left[\frac{1}{L} \sum_{j=1}^{L} \hat{U}_{i,j,n}{}^{3} \right]^{1/3} \quad (2)$$

3. Calculate mean value of the respective data sources (e.g. power, thrust, rot. speed)
4. Sort these values into the corresponding flow velocity bins
5. Calculate mean value for each flow velocity bin, *i*.
6. Sort the time averaged data into operating (producing power), free-wheeling, or parked (brake applied).

Mean bin equations for velocity *v*, electrical power P_{el}, thrust *T*, torque *M* and rotational speed *n* are given below. Each bin increment was chosen as 0.05 m/s.

$$\bar{U}_i = \frac{1}{N_i} \sum_{n=1}^{N_i} \bar{U}_{i,n} \quad (3)$$

$$\bar{P}_{el,i} = \frac{1}{N_i} \sum_{n=1}^{N_i} \bar{P}_{el,i,n} \quad (4)$$

$$\bar{T}_i = \frac{1}{N_i} \sum_{n=1}^{N_i} \bar{T}_{i,n} \quad (5)$$

$$\bar{M}_i = \frac{1}{N_i} \sum_{n=1}^{N_i} \bar{M}_{i,n} \quad (6)$$

$$\bar{n}_i = \frac{1}{N_i} \sum_{n=1}^{N_i} \bar{n}_{i,n} \quad (7)$$

B. Turbine Parameters

As per IEC the water-to-wire efficiency is defined as

$$\eta_{System,i} = \frac{\bar{P}_{el,i}}{\frac{1}{2}\rho A \bar{U}_i^3} \quad (8)$$

The mechanical power, P_m, is derived from equation 8 using a drive train and electrical system efficiency. With that the power coefficient c_p is calculated. A constant water density of ρ = 1025 kg/m^3 was used. The area, *A*, is the swept area of the rotor.

$$P_m = \frac{\bar{P}_{el,i}}{\eta_{drivetrain}\eta_{el\,system}} \quad (9)$$

$$c_P = \frac{P_{mech}}{\frac{1}{2}\rho A \bar{U}_i^3} \quad (10)$$

The thrust coefficient, c_T, is also calculated using the thrust, *T*, and the same parameters as the power coefficient calculation. The tip speed ratio, λ, is determined using the inflow velocity, angular velocity, ω, and rotor radius, *R*.

$$c_T = \frac{\bar{T}_i}{\frac{1}{2}\rho A \bar{U}_i^2} \quad (11)$$

$$\lambda = \frac{\omega R}{\bar{U}_i} \quad (12)$$

The thrust is calculated from the reaction force at the SIT Deployment Module (SDM) connection. This is determined from the force balance resolved about the SDM hinge point. The calculated force includes drag on the structure and rotor and so is denoted *Fx*, force in the axial, *x*, direction.

B. Turbulence

Velocity fluctuations are quantified in terms of turbulence intensity, *TI*. This is defined as the fluctuating part of the velocity divided by the mean velocity: The turbulence intensity at the current meter for each data set within each velocity bin was calculated.

$$TI = \frac{U_i'}{\overline{U_i}} \,. \qquad (13)$$

V. Results

A. Turbulence Intensity

A turbulence intensity (*TI*) scatter graph was derived using the bin method from the three consecutive days in December. The turbulence intensity can be seen to increase with velocity, leading to very high mean *TI*, over 40%, for flow speeds above 2m/s. This is contrary to other tidal sites [4]. This emphasises the special conditions in the wake of the Falls of Lora and quantifies the high temporal variation in flow that the turbines are operating in.

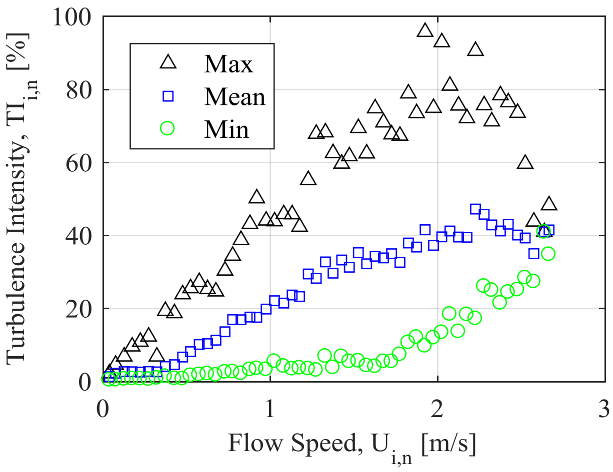

Figure 8: Turbulence Intensity (mean, minimum, maximum)

B. Time Varying Results

A time series of three days, in Figure 9, shows inflow velocity, power and load pin reaction with a 1Hz sampling frequency; this is shown for SIT2. It clearly indicates that the ebb is very dominant at the deployment site, hence power generation was limited to ebb, as well as daylight operations. This results in high power and reaction load (and thus thrust) output for one cycle per day. Overnight, the turbines were in parked mode, resulting in smaller thrust and drag forces compared to operational state.

Overall the high fluctuations in flow result in high fluctuations in power and thrust as well. Figure 10 shows a 1Hz sample time series over approximately one hour during December 19th, with a mean flow velocity of 1.9 m/s. High fluctuations of approximately ±1m/s can be seen.

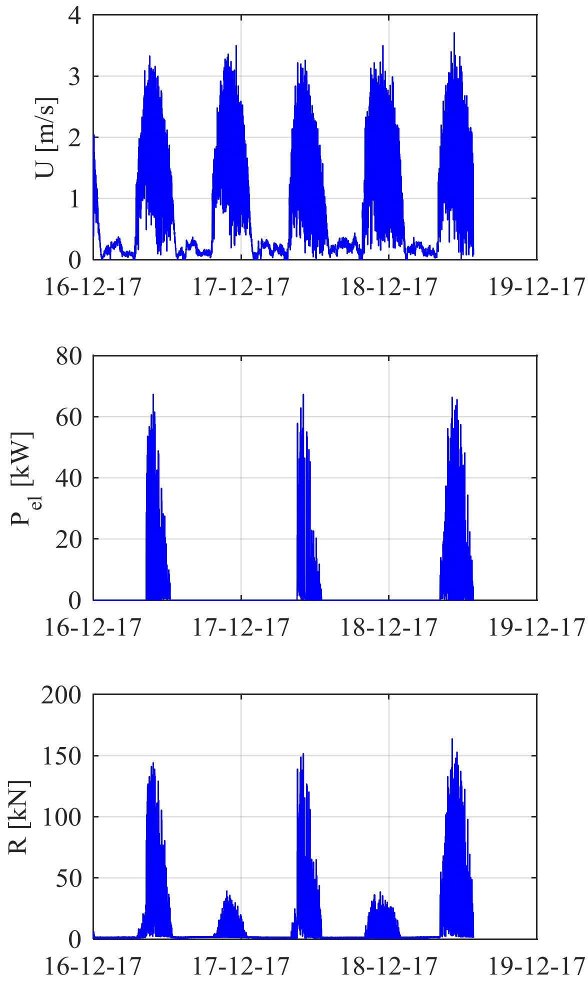

Figure 9: Raw Data Inflow velocity and turbine performance (SIT2 only)

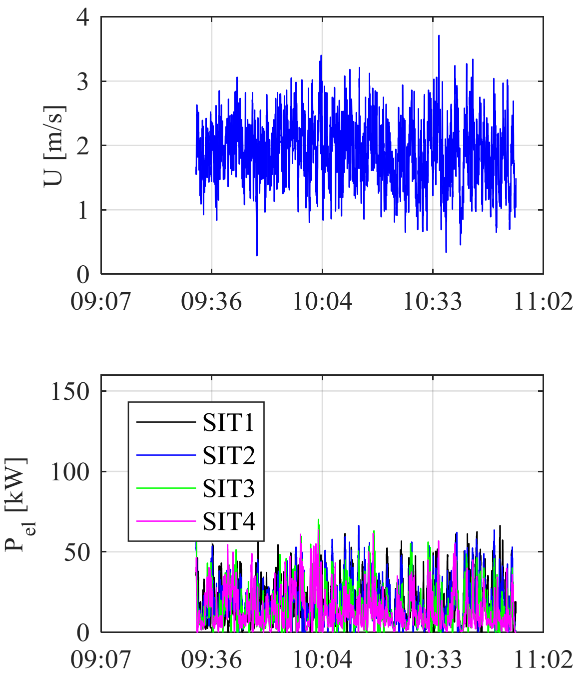

Figure 10: Sample Raw Data: Inflow velocity and turbine power (18/12/2017)

This also results in fluctuations in the turbines' output power, since they respond individually to the inflow variation due to their low inertia. Large differences are clear for the different turbines, indicating a spatial variation in inflow over the entire platform as well.

C. Performance Curves

The power curves for each turbine based on the IEC method are shown in Figure 11. On the Starboard side (SITs 3&4) the flow is more benign. The Starboard rotors do experience strong flows and have achieved rated power, but the flow speed is generally lower. The velocity measurement, the ECM, is located directly upstream from SIT2, in the stronger flow. For a given velocity SIT1 will therefore produce higher power and SITs 3&4 will produce lower power, creating the shift in the power curve.

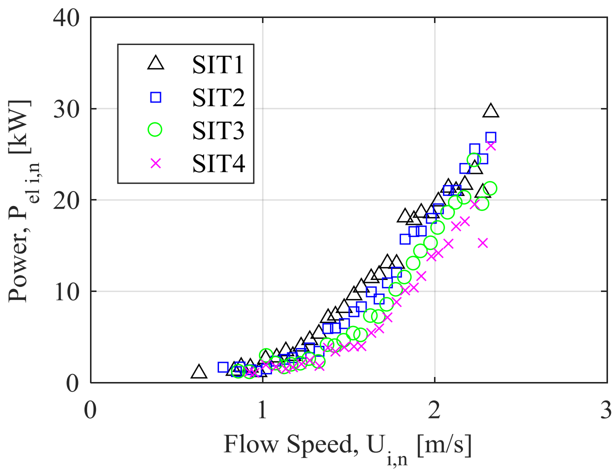

Figure 11: Individual turbine power output against inflow velocity

Only data from the December/January period is used. The results show that the power curves follow the same trend for each turbine, though they are shifted vertically, with SITs 1 and 2 producing more power than SITs 3 and 4. This is because there is spatial variation in flow speed across the platform. Figure 12 shows that the platform is not directly downstream from the Falls of Lora jet, due to licensing constraints, and so the Port turbines (SITs 1&2) are in faster flow that creates more turbulence and wake, which can be seen in the photo.

Some scatter from the cubic shape of the curves is also obvious for the higher flow speeds. This is because there are limited data sets in those higher velocity bins for v > 2.1m/s, as shown in Figure 13. There are high bin counts for flow speeds between approximately 1m/s and 2.1m/s, giving high confidence in these results.

Figure 12: Spatial variation of flow at site

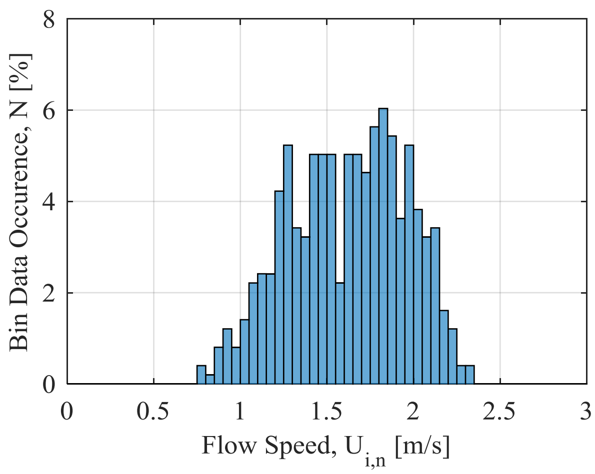

Figure 13: Histogram of data sets per velocity bin (exemplary for SIT2)

Fehler! Verweisquelle konnte nicht gefunden werden. presents the overall water-wire system efficiency, including all mechanical and electrical losses as per IEC [2].

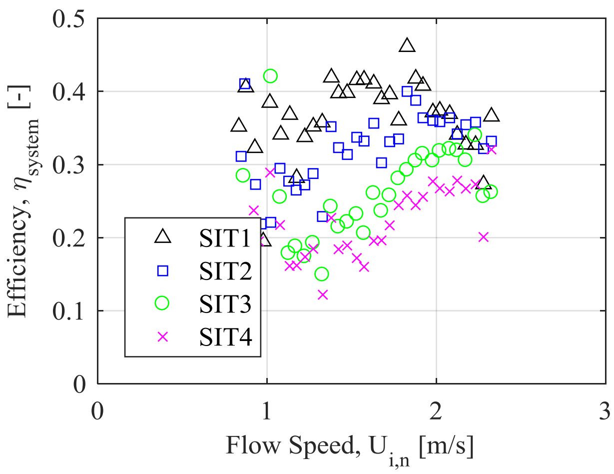

Figure 14: System efficiency against inflow velocity

As already discussed for the power curves, the same variation can be seen for the individual turbines because of the spatial variation and the position of the ECM. For SIT2 (being the turbine closest to the ECM) the system efficiency ranges between 0.3 - 0.37 for an inflow speed between 1.3 m/s and 2.3 m/s.

The resulting thrust curves from the turbines are shown in Figure 15. The same scatter for higher flow speeds is obvious as for the power curves before. Furthermore SITs 1 and 3 create more thrust than SITs 2 and 4. This is contrary to the trend in the power curves. In order to be independent from the velocity measurement and focus on the individual turbine characteristic Figure 16 shows turbine thrust against turbine power. Assuming that each turbine operates using the same torque-speed control strategy, as shown in Figure 17, one would expect to also see a collapsed result on a single curve for the thrust-power curve. This is the case for SITs 1 and 3, however SITs 2 and 4 show a lower thrust/power ratio. This will be further investigated in Part 2.

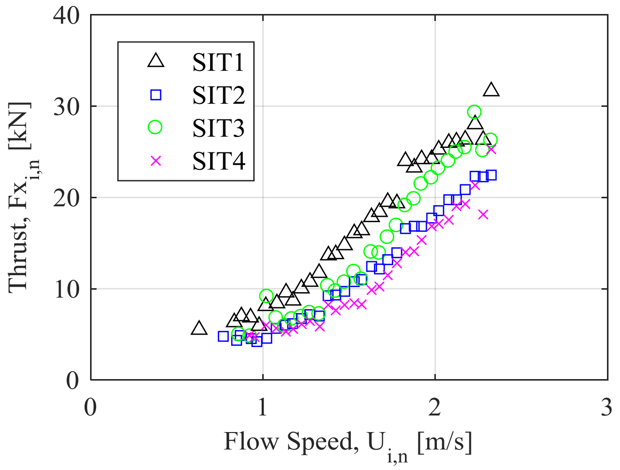

Figure 15: Turbine thrust against inflow velocity

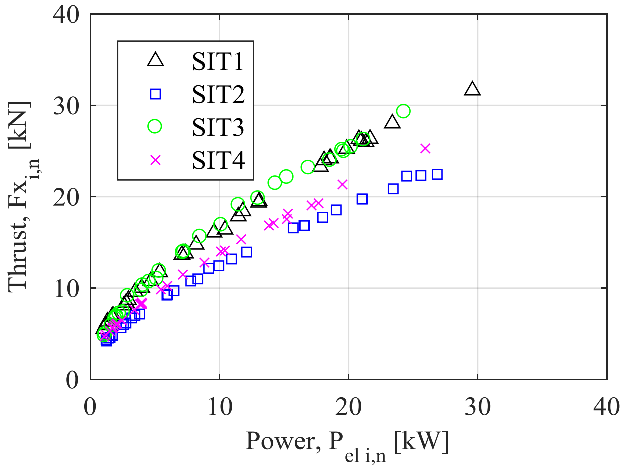

Figure 16: Turbine thrust against turbine power

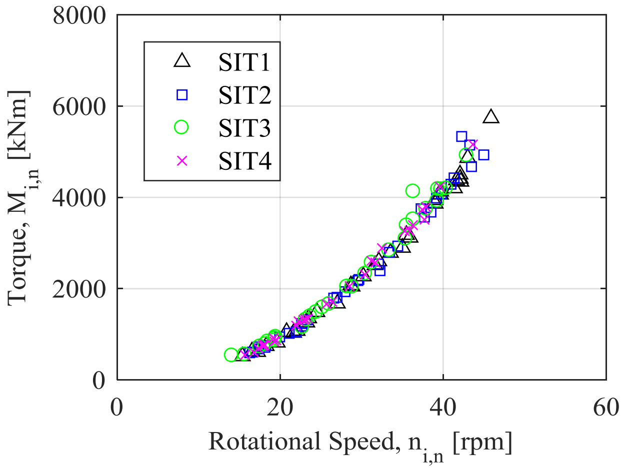

Figure 17: Turbine torque against turbine speed

E. Design Validation

In order to compare the field results with design predictions, a blade-element momentum method (BEM) as described and validated with model-scale tests in [1] is used. The BEM prediction also includes the steady state control curves for the turbine. The ECM is located directly upstream from SIT2 and due to the high spatial variation across the platform as discussed before only results for SIT2 are considered hereafter. Data from February is used in this section only, as the turbine has the same control parameters as that used in the BEM modelling. Figure 18 shows a comparison between measured power curve from SIT2 and the BEM prediction and thrust performance results are shown in Figure 19. Throughout the velocity range the prediction matches the measured full-scale data. The power curve result is very comparable, whereas the thrust is marginally higher in the field than the BEM model. This is because the drag of the SDM and nacelle, though very low, are included in the measured data. Though the SIT2 results show good comparison, the variation observed in Figure 15 will be further investigated.

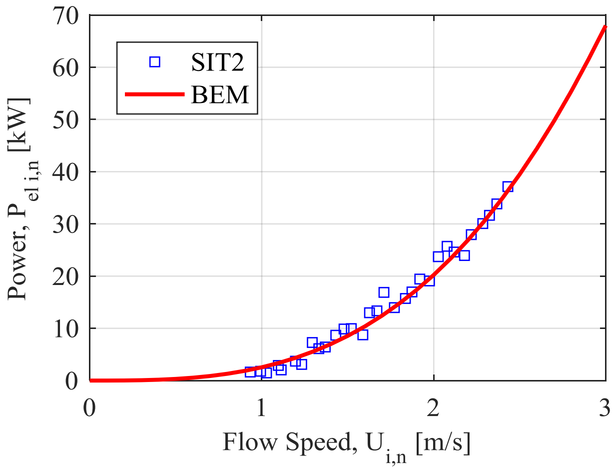

Figure 18: Turbine power against inflow velocity (SIT2)

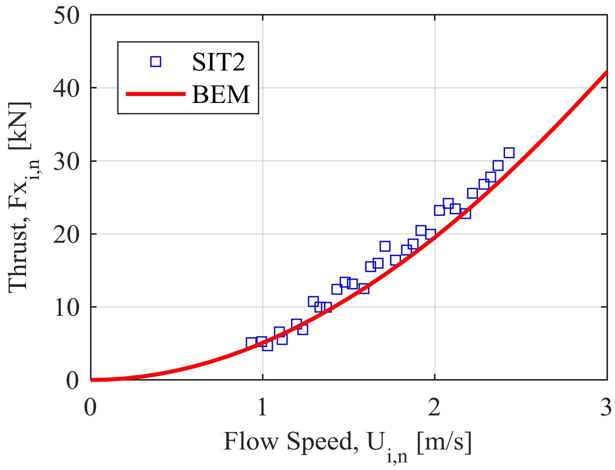

Figure 19: Turbine thrust against inflow velocity (SIT2)

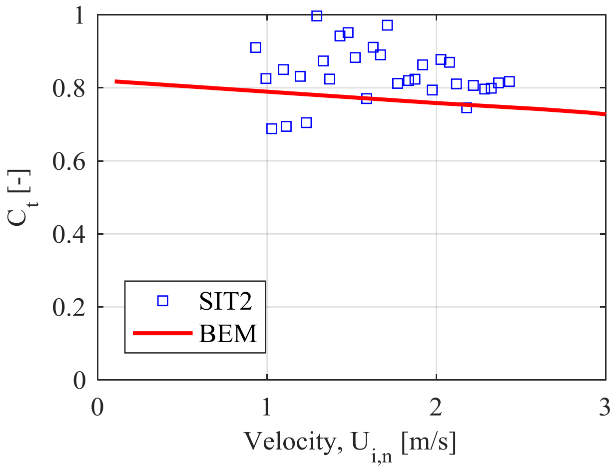

Figure 21: Rotor thrust performance against inflow velocity (SIT2)

Turbine performance coefficients in terms of non-dimensional values are evaluated for both power and thrust in Figure 20 and Figure 21. The measured performance coefficient c_p ranges from 0.4 - 0.5 for flow speeds above 1.3m/s. This is in good agreement with the BEM prediction. In the non-dimensional thrust curve, the measured thrust coefficient is higher than the BEM prediction, though still close, since it includes drag. The operating point in which the turbine is working in terms of its tip speed ratio (*TSR*) is shown in Figure 22. It is clear, that the turbine is operating at its design *TSR* when at optimal c_p.

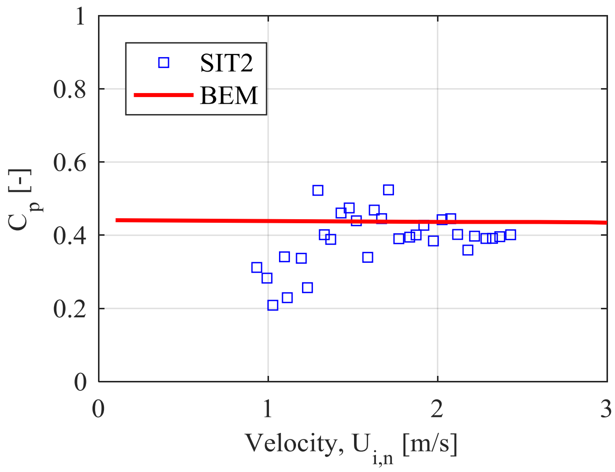

Figure 20: Rotor power performance against inflow velocity (SIT2)

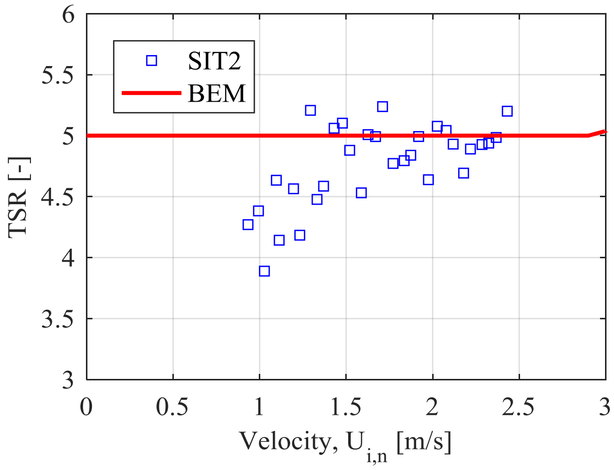

Figure 22: Rotor tip speed ratio against inflow velocity (SIT2)

VI. Summary and Conclusion

Field testing of four SIT turbines mounted on a floating PLAT-I platform has been carried out in Connel, Scotland. The test site downstream from the Falls of Lora shows a very high spatial and temporal variation in inflow speed with mean turbulence intensities of 40% at 2m/s. Post processing according to IEC 62600-200 has been used to evaluate the individual turbine performance.

Using a single velocity measurement location, the spatial variation in inflow creates a shift in the individual turbine performance curves, depending on proximity to the velocity measurement. Future work will include analysis of multiple velocity instruments around the platform (including seabed and vessel mounted ADCPs) to further analyse the effect of proximity, as well as possibly providing recommendations to the review team of IEC 62600-200.

The measured thrust/power ratio varies across the turbines, although they are running on the same control curves.

Therefore, the thrust measurement using the load pins is currently being reviewed and is further detailed in Part 2.

Power performance for SIT2, the turbine located closest to the velocity measurement, shows perfect agreement with semi-empirical power and thrust (taking into account drag) predictions using BEM. In general, the results derived from the testing provide a high level of design confidence in the turbines' performance.

ACKNOWLEDGEMENTS

This work has been supported by the Federal Ministry for Economic Affairs and Energy of Germany (BMWi) in the project TIDAL POWER (FKZ 0325817B) and the EPSRC funded SURFTEC (SUrvivability and Reliability of Floating Tidal Energy Converters) project (EP/N02057X/1).

REFERENCES

[1] N. Kaufmann, T.H. Carolus, R. Starzmann, "An enhanced and validated performance and cavitation prediction model for horizontal axis tidal turbines", *International Journal of Marine Energy*, Volume 19, pages 145-163, 2017.

[2] *Marine energy – Wave, tidal and other water current converters – Part 200: Electricity producing tidal energy converters – Power performance assessment,* IEC/TS 62600-200, 2014.

[3] J. McNaughton, S. Harper, R. Sinclair, and B. Sellar, "Measuring and modelling the power curve of a Commercial-Scale tidal turbine", In *Proc. of 11th EWTEC*, Nantes, France, 6-11 Sept 2015.

[4] R. Starzmann, M. Baldus, E. Groh, N. Hirsch and N. Lange, "Full-Scale Testing of a Tidal Energy Converter using a Tug Boat", In *Proc. of 10th EWTEC*, Aalborg, Denmark, 2-5 Sept 2013.

[5] P. Jeffcoate, R. Starzmann, B. Elsaesser, S. Scholl and S. Bischof, "Field Measurements of a Full Scale Tidal Turbine", *International Journal of Marine Energy*, Volume 12, pages 3-20, 2015.

[6] R. Starzmann, P. Jeffcoate, S. Scholl, S. Bischof, and B. Elsaesser, "Field testing a full-scale tidal turbine Part 1: Power Performance Assessment", In *Proc. of 11th EWTEC*, Nantes, France, 6-11 Sept 2015.

[7] P. Jeffcoate, N. Cresswell, "Field Performance Testing of a Floating Tidal Energy Platform - Part 2: Load Performance", In *Proc. of 4th AWTEC*, Taipei, Taiwan, 9-13 Sept 2018.